

## Probe induced secondary Voids in Complex Plasmas under Microgravity

M. Klindworth<sup>1</sup>, A. Piel<sup>1</sup>, A. Melzer<sup>2</sup>, U. Konopka<sup>3</sup>,  
H. Roethermel<sup>3</sup>, K. Tarantik<sup>3</sup> and G. E. Morfill<sup>3</sup>

<sup>1</sup> *Institut für Experimentelle und Angewandte Physik, Christian-Albrechts-Universität Kiel, 24098 Kiel, Germany*

<sup>2</sup> *Institut für Physik, Ernst-Moritz-Arndt-Universität, 17489 Greifswald, Germany*

<sup>3</sup> *Centre for Interdisciplinary Plasma Science, Max-Planck-Institut für Extraterrestrische Physik, 85740 Garching, Germany*

### Abstract

Dust particles are found to settle in the presheath of a floating body in a plasma under microgravity conditions, where an equilibrium of the electric field force and ion drag force establishes. The size and shape of the shell-like dust formation can be quantitatively explained by a combined model for the presheath and the ion drag. The model also yields the force gradients of the formed confining potential, which are responsible for the formation of distinct particle layers in the dust arrangement.

### Experiment and Observations

Complex (dusty) plasmas consist of electrons, ions and micrometer sized particles, that charge up negatively when immersed into the discharge. A number of phenomena, unknown from ordinary plasma, are observed in complex plasmas, for example the formation of a central dust-free region (“void”) that has been observed in experiments and simulations (e.g. [1]). The void is understood as an effect of the ion drag, exerting an outward directed force on the particles and the electric field force, that confines the negative dust grains in the positive plasma bulk. Here, a novel approach to study void phenomena is presented, which relates to the recent discussion on the influence of Debye shielding on the ion drag force [2, 3]. Micrometer sized

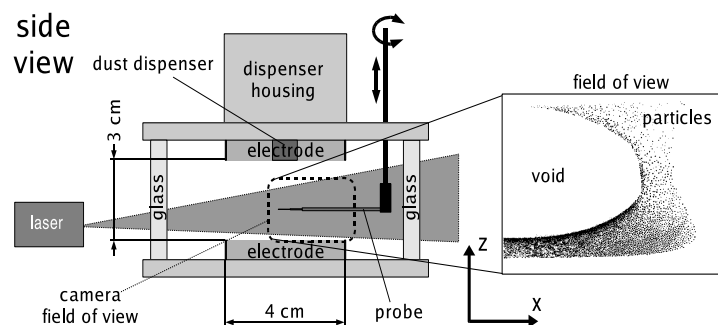


Figure 1: Scheme of the PKE plasma chamber with the field of view of the camera, showing a typical dust arrangement with a central void-region under microgravity.

particles settle, under typical laboratory conditions, in the lower sheath of a plasma, which is a result of their non-negligible weight. Under microgravity the dust fills the volume and

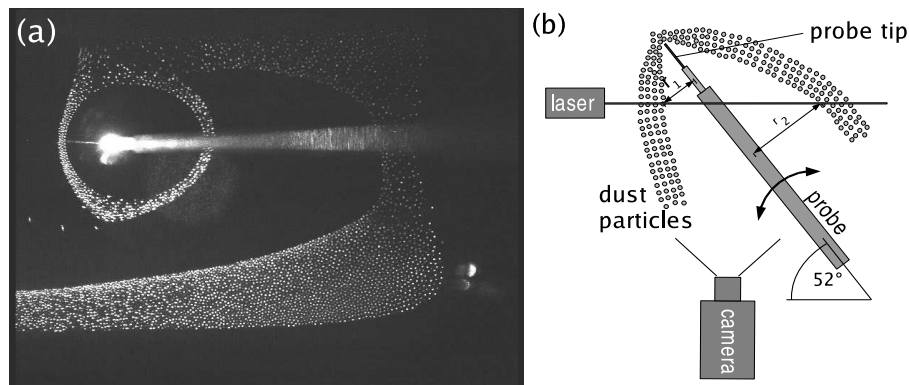


Figure 2: (a) Video image of the observation camera. Dust particles appearing as a ring around the probe inside the central void in the plasma. (b) Scheme of the observation geometry and the intersecting laser sheet from the top.

voids can be studied. The experimental setup (Fig. 1) comprises of a capacitively coupled rf plasma chamber (PKE vessel) with two electrodes of 40 mm diameter and a gap of 30 mm. Typical argon discharge parameters are 40 Pa pressure and 80 V<sub>pp</sub> rf voltage at 13.56 MHz. The immersed plastic particles have a diameter of 3.4 μm. To measure plasma parameter profiles, a Langmuir probe scans a 2D cross section of the discharge. Besides the tip of 4 mm length and 25 μm radius, the probe design includes a large area reference electrode for passive rf compensation. Trapped particles in the plasma are illuminated by a laser fan and observed with a CCD camera.

In the experiments under microgravity conditions, a large void is formed in the center of the bulk-plasma (see Fig. 1,2(a)). When the probe shaft traverses the surrounding dust cloud to operate inside the void, a large amount of dust is trapped around the probe and appears like a dust ring in the intersecting laser light (Fig. 2(a)). The ring forms a secondary void inside the large void structure. Rotating the probe the laser intersection point moves along the probe shaft and allows to determine the radius of the dust ring, which is plotted in Fig. 3(a). Obviously, the particles form a hollow conical sleeve. Additionally, the thin shell of the dust cloud consists of 3-4 distinct particle layers. The formation of layers in narrow confinements has also been observed in [4, 5]. Since most parts of the probe shaft are insulated and therefore biased to the floating potential, the influence of the applied measuring voltage (-40 V to +80 V) is only visible close to the tip of the probe. The dust cloud around the probe tip collapses, as soon as the probe bias exceeds the plasma potential, which is explained by attraction of the negative dust particles.

## Numerical Model and Discussion

From the equality of electron and ion current to the floating parts of the probe the radial position of the sheath edge around the probe can be approximated. In Fig. 3 the sheath edge is

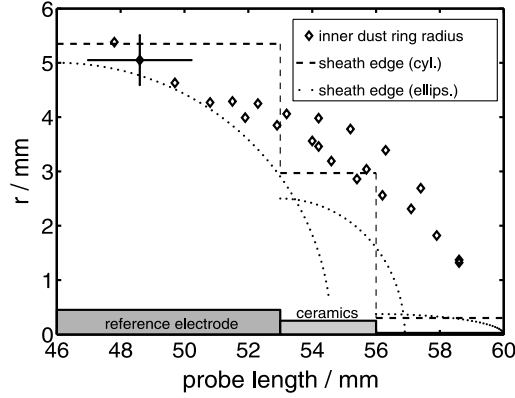


Figure 3: (a) Inner radius of the dust shell around the probe. The dashed/dotted lines mark the theoretical sheath edge positions with respect to the radius of the probe part. The probe tip covers the length 56-60 mm. (b) Outer and inner radius of the shell close to the probe tip, probe bias  $V_p$  and measured plasma potential  $\phi_p$  versus time.

marked (a) assuming strictly radial ion motion to the probe, which results in a cylindrically shaped sheath and (b) for a spheroidal shape as suggested in [6]. Since the dust is located outside the sheath, but close to its edge, where the approaching ions are already accelerated to reach Bohm velocity at the sheath edge, the ion drag force is suggested to balance the repulsive electric field force on the grains, that is caused by the floating potential of the probe shaft.

Arguing, that the spheroidal potential contour lines around a finite cylindrical probes become nearly spherical at distances larger than the probe length, the electric field and ion velocity is derived from the solution of a presheath model for spherical probes [6]. The model accounts for weak ion-neutral collisionality, that is evident under the given experiment conditions. The ion drag force has been determined for the Barnes model [7] and Khrapak's model

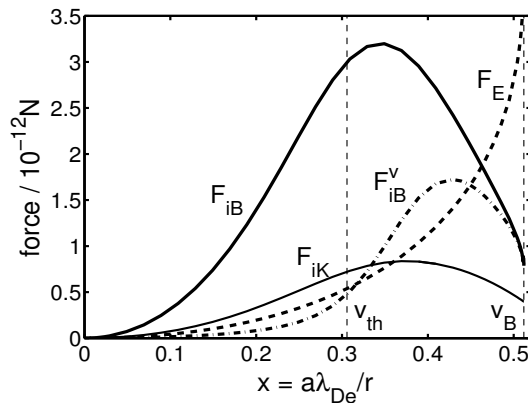


Figure 4: The electric field force  $F_E$  and the corresponding ion drag forces after the different models: Barnes's model [7] with a Coulomb cut-off radius of  $0.7 \cdot \lambda_{De}$  ( $F_{iB}$ ), with an ion velocity dependent cut-off radius ( $F_{iB}^v$ ) and Khrapak's model ( $F_{iK}$ ) [2]. Vertical lines indicate at which radial coordinate  $x$  the ions reach the thermal velocity  $v_{th}$  and Bohm velocity  $v_B$ .

[2]. The drag force after [7] has been calculated for two different Coulomb cut-off radii: first

with the Debye length as function of the ion velocity  $v_i$ ,

$$\lambda_D(v_i) = \left( \frac{1}{\lambda_{De}^2} + \frac{1}{\lambda_{Di}^2} \frac{1}{(1 + v_i^2/v_{th}^2)} \right)^{-1/2}, \quad (1)$$

where  $\lambda_{De,Di}$  are the electron and ion Debye length and  $v_{th}$  is the thermal ion velocity. Thus,  $\lambda_D(v_i)$  takes into account the directed ion motion in the presheath in addition to their thermal motion. With respect to the common use of  $\lambda_{De}$  as cut-off radius, the second calculation includes a fixed value of  $\lambda_D(v_i = v_B)$ . All forces have been evaluated under the assumption of a fixed particle charge, which is derived from the OML model. The magnitudes of the resulting forces close to the insulating ceramics of the probe are plotted in Fig.4 as function of the  $x = a\lambda_{De}/r$  with the radial distance  $r$  and normalized ion current  $a$ . It is seen, that the electric field force intersects the ion drag force at subsonic ion velocities, what agrees with the first approximation above. The equilibrium positions for the different ion drag models are found at  $r_{iB} = 3.5$  mm,  $r_{iB}^v = 3.6$  mm and  $r_{iK} = 4.4$  mm, while the sheath edge is located at a radial distance of 3.1 mm from the probe. The calculations match the observations in Fig. 3(a).

Summarizing, the particle trapping visualizes the sheath edge around an object in the plasma and introduces a new method to study the mechanism, on which the void phenomenon is based.

#### Acknowledgments

The Kiel investigations were supported by DLR under contract 50WM0039. U. Konopka is supported by DLR under contract 50WP0203.

- [1] Morfill, G. E., Thomas, H. M., Konopka, U., Rothermel, H., Zuzic, M., Ivlev, A., and Goree, J., *Phys. Rev. Lett.*, **83**, 1598–1601 (1999).
- [2] Khrapak, S. A., Ivlev, A. V., Morfill, G. E., and Thomas, H. M., *Phys. Rev. E*, **66**, 046414 (2002).
- [3] Zafiu, C., Melzer, A., and Piel, A., *Phys. Plasmas*, **10**, 4582–4583 (2003).
- [4] Teng, L.-W., Tu, P.-S., and I, L., *Phys. Rev. Lett.*, **90**, 245004 (2003).
- [5] Totsuji, H., Kishimoto, T., and Totsuji, C., *Phys. Rev. Lett.*, **78**, 3113–3116 (1997).
- [6] Bryant, P., Dyson, A., and Allen, J. E., *Journal of Physics D: Applied Physics*, **34**, 1491–1498 (2001).
- [7] Barnes, M. S., Keller, J. H., Forster, J. C., O'Neill, J. A., and Coultas, D. K., *Phys. Rev. Lett.*, **68**, 313–316 (1992).